Solid-State Radiometer Measurements of Sea Surface Skin Temperature

C. J. DONLON,* S. J. KEOGH,+ D. J. BALDWIN,+ I. S. ROBINSON,+ I. RIDLEY,# T. SHEASBY,#
I. J. BARTON,@ E. F. BRADLEY,& T. J. NIGHTINGALE,**AND W. EMERY*

* *Colorado Center for Astrodynamics Research, University of Colorado, Boulder, Colorado*
+ *Southampton Oceanography Center, University of Southampton, Southampton, United Kingdom*
# *University of Leicester, Leicester, United Kingdom*
@ *CSIRO Division of Atmospheric Research, Aspendale, Victoria, Australia*
& *CSIRO Black Mountain Labs, Canberra, Australia*
** *Rutherford Appleton Laboratory, Oxford, United Kingdom*

(Manuscript received 5 May 1997, in final form 25 August 1997)

ABSTRACT

Satellite sea surface skin temperature (SSST) maps are readily available from precisely calibrated radiometer systems such as the ERS along-track scanning radiometer and, in the near future, from the moderate-resolution imaging spectroradiometer. However, the use of subsurface bulk sea surface temperature (BSST) measurements as the primary source of in situ data required for the development of new sea surface temperature algorithms and the accurate validation of these global datasets is questionable. This is because BSST measurements are not a measure of the sea surface skin temperature, which is actually observed by a satellite infrared radiometer. Consequently, the use of BSST data for validation and derivation of satellite derived ''pseudo-BSST'' and SSST datasets will limit their accuracy to at least the rms deviation of the BSST–SSST difference, typically about ± 0.5 K. Unfortunately, the prohibitive cost and difficulty of deploying infrared radiometers at sea has prevented the regular collection of a comprehensive global satellite SSST validation dataset. In response to this situation, an assessment of the TASCO THI-500L infrared radiometer system as a potential candidate for the widespread validation of satellite SSST observations is presented. This is a low-cost, broadband radiometer that has been commonly deployed in the field to measure SSST by several research groups. A comparison between SSST derived from TASCO THI-500L measurements and contemporaneous scanning infrared sea surface temperature radiometer measurements, which are accurate to better than 0.1 K, demonstrates low bias (0.1 K) and rms (0.08 K) differences between the two instruments. However, to achieve this accuracy, the TASCO THI-500L radiometer must be deployed with care to ensure that the radiometer fore-optics are kept free of salt water contamination and shaded from direct sunlight. When this is done, this type of low-cost radiometer system could form the core of a global SSST validation program.

1. Introduction

Satellite sea surface skin temperature (SSST) maps are now readily available from the precisely calibrated *ERS-1* and *-2* along-track scanning radiometers (ATSRs) (Edwards et al. 1990) and, in the near future, from the advanced ATSR (AATSR) and the moderate resolution imaging spectroradiometer (MODIS) systems. Such infrared radiometers measure the sea surface temperature (SST) from a thin ''skin'' surface layer, having a depth equal to the *e*-folding attenuation length of infrared radiation in seawater (at a wavelength of 10 μm this equates to a depth of approximately 10 μm). Subsurface bulk SST (BSST) measurements can be significantly decoupled from the SSST because of diurnal warming events in the daytime and the cool skin temperature deviation at night. Temperature variations greater than 1 K are typical of a diurnal warming events (e.g., Yokoyama and Tanba 1991), and variations of the order ± 1 K are experienced in the thin skin layer (e.g., Donlon and Robinson 1997; Kent et al. 1996; Schlüssel et al. 1990). Consequently, the accuracy of satellite SSST or ''pseudo-BSST'' algorithms (an infrared measurement of SST can only infer a true BSST from an SSST observation) derived and validated using BSST measurements will always be limited to at least the rms value of the BSST–SSST temperature difference, which is typically about ± 0.5 K. Further, the use of BSST validation data will also impose a mean cool bias equal to the magnitude of the BSST–SSST difference (approximately 0.35 K) to the satellite-derived SSST. These significant error estimates are independent of the success to which current satellite radiometer multiview and multispectral techniques can compensate for the effect of the intervening atmosphere.

Corresponding author address: Dr. Craig J. Donlon, Colorado Center for Astrodynamics Research (CCAR), University of Colorado, Campus Box 431, Boulder, CO 80309-0431.
E-mail: cjdn@colorado.edu

TABLE 1. The main characteristics of the TASCO THI-500L radiometer when equipped with a THI-PRL head unit and the RAL SISTeR radiometer.

Instrument	TASCO THI-500L	RAL SISTeR
Spectral response	8–12 μm	10.8 μm $\pm$ 0.5 μm
Measurement range	205–770 K	100–400 K
Resolution	1 mV K^{-1}	N/A
ϵ range	0.1–1.0 in 0.01 intervals	N/A
Beam half-angle	4.3°	6.5°
Response time	1.5 s	100 ms*
MEU dimensions	140 $\times$ 72 $\times$ 34 mm	N/A
THI-PRL dimensions	140 $\times$ 29 $\times$ 34 mm	N/A

* One period of the internal chopper. Intervals can be programmed in 100-ms increments.

One acceptable approach to validate satellite SSST observations using BSST observations is to use only satellite–buoy observations collected in high wind speed (greater than 10 m s^{-1}) conditions. In these cases, the wind-induced turbulence at the air–sea interface dominates the heat exchange between the ocean and atmosphere; even at high total heat flux values the surface renewal is extremely rapid, and turbulent heat transfer dominates the air–sea interface. In such conditions, the skin temperature deviation is negligible (Donlon and Robinson 1997), and the BSST is directly comparable to an infrared satellite observation. Further, during clear-sky conditions and strong solar warming, wind speeds greater than 4 m s^{-1} prevent the formation of a diurnal layer eliminating this complicating feature from the validation dataset (e.g., Emery et al. 1996). Unfortunately, high wind speed conditions do not prevail across the global ocean, and in situ radiometer measurements coincident in space and time with satellite observations are still required to validate a satellite-derived SSST. The widespread use of in situ research instrumentation, such as the scanning infrared sea surface temperature radiometer (SISTeR) (Nightingale 1997) or the modified-atmospheric emitted radiance interferometer (M-AERI) (Smith et al. 1997; Rivercombe et al. 1993), is limited both financially and practically. Thus, there is a need to explore different strategies for the ongoing validation and calibration of satellite-derived SSST and pseudo-BSST datasets, as discussed by Thomas and Turner (1995).

This paper presents an evaluation of a low-cost, broadband, single-channel infrared radiometer system (TASCO THI-500L) as a potential candidate for the widespread global validation of satellite-derived SSST and pseudo-BSST datasets. The following sections describe the methodology used to obtain SSST observations from TASCO THI-500L brightness temperature measurements. Several different in situ datasets are then used to explore both the deficiencies and advantages of the TASCO THI-500L system to measure SSST. Finally, we present our conclusions and recommendations for future deployments of these instruments.

2. Description of the TASCO THI-500L radiometer

The TASCO THI-500L radiometer is an ''off-the-shelf'' portable broadband narrow beam radiometer consisting of a main electronics unit (MEU) and a separate detector head unit (THI-PRL). The MEU has a small keypad and display screen that is used to set a number of measurement parameters, including values for the target emissivity and the measurement integration period. The MEU can be powered either from batteries or from a separate DC supply for longer deployments. An analog output is taken from the MEU via a dedicated socket providing a 1 mV K^{-1} output signal. Although several detector head units are available for the MEU, the narrow spectral response of the THI-PRL head is best suited to the measurement of SSST because the atmospheric transmission in this spectral region is high. The THI-PRL houses the detector element and associated electronics in a small cylinder that is connected to the MEU via a single cable. The detector is mounted behind a lens that focuses radiation collected from a divergent beam having a half-angle of 4.3°, which, for a typical pathlength of 10 m, equates to a 1.5-m circular field of view. The main specifications of the TASCO THI-500L radiometer and THI-PRL detector head are summarized in Table 1. For comparison, the specifications of RAL SISTeR (Nightingale 1997) are also given.

The combined spectral response of the THI-PRL detector window and lens, provided by the instrument manufacturer, is presented in Fig. 1. The spectral response shows a sharp rise to peak transmission from 8.0 to 9.5 μm, followed by a steady fall in transmission up to a wavelength of 15.0 μm. For most of this spectral waveband, atmospheric absorption primarily due to the water vapor continuum is weak. In the case of satellite observations the effects of ozone centered at 9.6 μm, and CO_2 at wavelengths greater than 13.0 μm are significant (e.g., Závody et al. 1995). However, in the case of a ship-mounted instrument, these effects are negligible because of the small (typically less than 20 m) pathlength between the radiometer and sea surface of most ship installations.

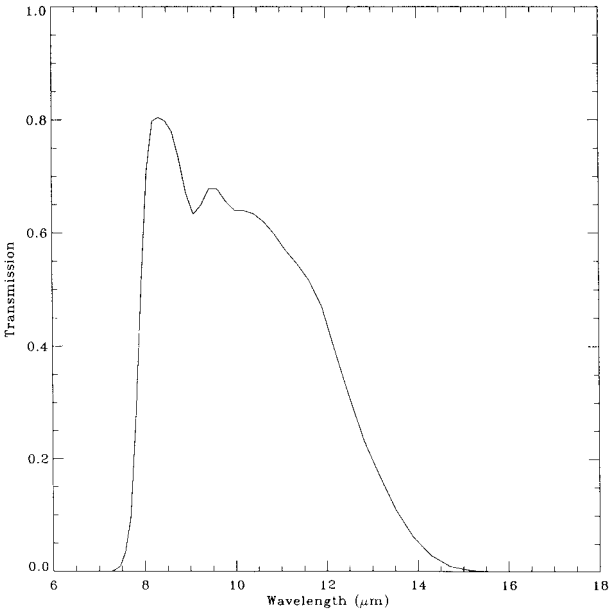

FIG. 1. The combined spectral response of the TASCO THI-500L detector window and lens filter. Data courtesy of TASCO Japan Co., Ltd.

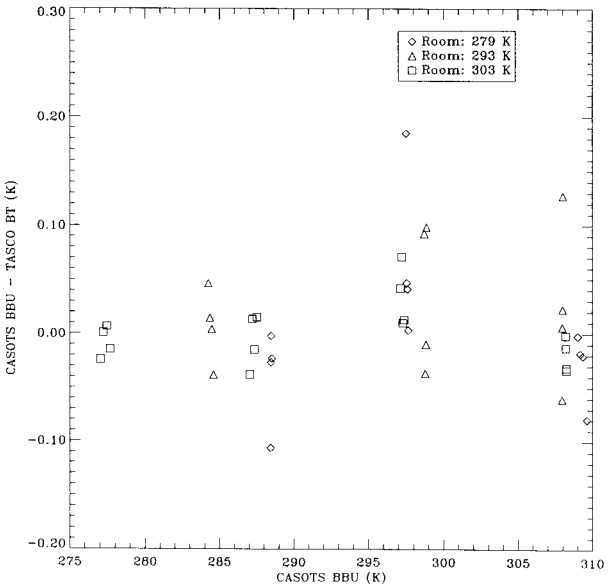

FIG. 2. The residual difference between the CASOTS blackbody temperature and radiometric temperatures derived from four different TASCO radiometers plotted as a function of CASOTS blackbody temperature. All data were obtained during the CASOTS 1996 workshop and include observation runs at three different environmental temperatures.

3. Laboratory calibration of the TASCO THI-500L radiometer

To determine the accuracy of a radiometer, an absolute calibration against an independent well-characterized radiance source of known temperature and emission characteristics is required. As the TASCO instrument does not have an internal calibration blackbody or mechanical chopper system, the effect of environmental temperature changes could significantly affect the instrument calibration. For this reason it is desirable to calibrate the radiometer at a variety of ambient temperatures typical of those expected in the field.

During the Combined Action for the Study of the Ocean Thermal Skin (CASOTS) radiometer intercalibration experiment (Donlon et al. 1998, manuscript submitted to *J. Atmos. Oceanic Technol.*), four separate TASCO THI-500L radiometers viewed a radiance source over a temperature range of 279–308 K while maintained at a steady environmental temperature. Calibrations were performed at environmental temperatures of 279, 293, and 303 K, which were chosen to simulate ''cold,'' ''ambient,'' and ''hot'' operating temperatures. The calibration blackbody used during this exercise was developed specifically for the calibration of seagoing infrared radiometers, which can be used both in the laboratory or in the field. The emissivity of this cavity for a spot radius of less than 30 mm is greater than 0.999, and during the CASOTS experiment, the temperature of the cavity was determined to an accuracy of 0.05 K. The reader is referred to Donlon et al. (1998, manuscript submitted to *J. Atmos. Oceanic Technol.*) for a full description of the CASOTS blackbody design and operation.

A composite plot of the residual difference between the CASOTS blackbody temperature and the output from the four TASCO instruments plotted as a function of the CASOTS blackbody temperature for hot, ambient, and cold environments is shown in Fig. 2. This figure clearly demonstrates the consistent performance of the TASCO THI-500L radiometers over the expected range of operating temperatures. In all cases the difference between TASCO and CASOTS blackbody is less than ± 0.2 K, and in all but one case[1] the agreement is better than ± 0.1 K. No relationship between the environment temperature and the residual is observed for any of the TASCO radiometers used during the CASOTS experiment. Based on these data, several field deployments have been undertaken by different research teams to assess the feasibility of using the TASCO THI-500L radiometer for the accurate and reliable measurement of in situ SSST suitable for the validation of satellite-derived SSST. These are discussed in the following sections.

4. Results from field deployments

Grassl and Hinzpeter (1975) first describe a radiometer calibration strategy that has been used by sev-

[1] This particular radiometer has been used extensively in the field and has a replacement lens.

eral authors to calibrate seagoing infrared radiometers (e.g., Saurez et al. 1997; Schlüssel et al. 1987; Schlüssel et al. 1990). In this scheme, the radiometer periodically views a vigorously stirred bath of seawater of known temperature. Assuming that stirring prevents any vertical or horizontal temperature gradients and that the environmental conditions remain constant throughout the calibration interval (typically about 1 min), the radiometer signal can be absolutely calibrated by relating the measured water bath temperature to the radiometer signal. One of the major benefits of this strategy is that the emissivity term falls out of the calibration exercise if seawater is used in the calibration bath, assuming that the effect of the different surface roughness features present on the sea surface and water bath are considered equal and that the sky conditions (cloud cover) do not change significantly in the time it takes to complete a calibration cycle.

A recent study (Zappa 1997) using thermal imagery to validate the stirred bath calibration method clearly show that the effect of ''wind'' gusts blowing over the surface of the stirred bath introduce a radiometric cool bias of approximately 0.1 K for typical ocean–atmosphere conditions relative to the bucket temperature, a feature also observed by the authors during a similar laboratory calibration experiment made during the Mutsu Bay experiment (Donlon et al. 1995). Further, the work of Yoshimori et al. (1994; 1995) clearly highlights the significant effect surface roughness can have on an SSST measurement. In this case the different wave slopes of the wave field reflect sky radiance from a large area of sky into the radiometer field of view. Consequently, we choose to compute the SSST using independent TASCO brightness temperature (BT) observations of the sea and sky radiance together with a computed seawater emissivity in order to account for the nonblackness of the sea surface.[2]

a. Seawater emissivity

It is important to have an accurate estimate of the seawater emissivity as a small emissivity change of approximately 0.01 has a significant effect on the derived SSST. The deviation of seawater emissivity (ϵ) from unity requires that reflected sky radiance be accounted for when using measurements of the seawater radiance to determine the actual SSST. This is done by compensating for the downwelling sky radiance contribution over the same spectral band as the sea view using an appropriate value for the seawater emissivity:

$$\mathrm{Rsea}_{\mathrm{true}} = \frac{[R_{\mathrm{sea}} - (1.0 - \epsilon) \times R_{\mathrm{sky}}]}{\epsilon}, \qquad (1)$$

where $\mathrm{Rsea}_{\mathrm{true}}$ is the seawater leaving radiance, R_{sea}, measured by the sea view radiometer corrected for reflection of the downwelling sky radiance R_{sky}, measured by the sky view radiometer, and ϵ is the seawater emissivity. The ϵ of the sea surface is wavelength and view angle dependent, as documented by Masuda et al. (1988) and Watts et al. (1996). This variation is shown in Fig. 3 over the spectral range of the TASCO THI-500L and for view angles ζ between 0° and 50°. Considering the broad spectral interval of the TASCO radiometer (Fig. 1), it is clear that the most appropriate ϵ value should be that which is integrated across the spectral bandwidth of the radiometer and weighted by the normalized transmission function of the instrument's foreoptics.

We use the planar seawater ϵ data of Masuda et al. (1988) and Downing and Williams (1975) interpolated to a uniform wavenumber spacing between 1250 and 830 cm^{-1}. These data are convolved with the normalized combined filter and detector transmission curve shown in Fig. 1 to provide a weighted ϵ value for the TASCO instrument. The results of this procedure are tabulated in Table 2 for ζ between 0° and 50°. Although Masuda et al. (1988) provide ϵ data for different wind speed and surface roughness conditions, the more recent work of Watts et al. (1996) suggests that secondary reflections at the sea surface limit the surface roughness effect on the value of ϵ below view angles of about 40°. Consequently, only a single ϵ value is tabulated for all wind speeds. Data for $\zeta > 50°$ are not given, as the increased sensitivity of ϵ to changes in ζ at large angles demands precise ship roll and pitch measurements. When such data are available, a correction may be made for the effects of ship roll and pitch, although great care must be taken to ensure that the roll and pitch data are of sufficient resolution and accuracy to make such a correction worthwhile. We recommend that this approach is avoided by limiting the instrument sea view to angles smaller than 50° from nadir.

The TASCO radiometer returns a voltage that is proportional to the BT of the target rather than a radiance value that is required when combining the sea and sky BT observations to account for the seawater emissivity. To simplify the conversion of BT to radiance, the integrated radiance of the TASCO THI-500L was calculated for a temperature range of 200–340 K using the normalized spectral response of the TASCO THI-500L illustrated in Fig. 1 and a polynomial function fitted to the resulting data. The computed radiance to temperature relationship is presented in Fig. 4, and the coefficients of the curve are given in Table 3. We also provide the polynomial coefficients for the inverse relationship across the expected range of both the sky and sea temperatures. However, to minimize the errors associated with the use of polynomial expansions (we note a radiance error of 0.08% equates to a temperature error of about 0.2 K), we recommend that direct in-

[2] Typically, two TASCO THI-500L radiometers are used contemporaneously for this purpose: one instrument views the sea surface and the second, the sky.

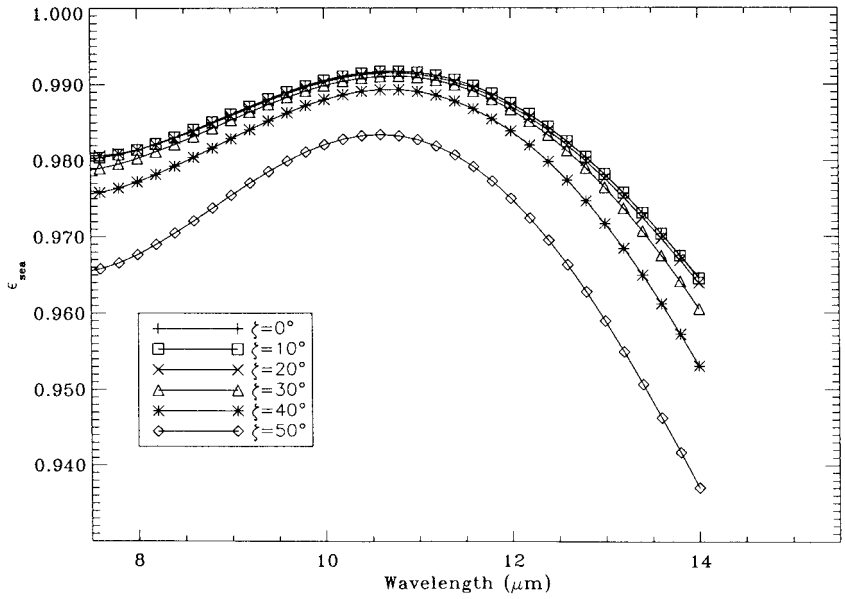

FIG. 3. Emissivity of seawater over the spectral bandwidth used by the TASCO THI-500L radiometer for different viewing geometries. Data from Masuda et al. (1988) and Downing and Williams (1975).

version of the coefficients is undertaken using an appropriate technique (e.g., the Newton–Ralphson method).

b. Results from the 1996 ROSSA–AMT-3 experiment

During the joint Radiometric Observations of the Sea Surface and Atmosphere (Donlon 1997) and Atlantic Meridional Transect-3 experiment (Bale 1997), two TASCO THI-500L radiometers were operated from the forward mast of the RRS *James Clark Ross* on a transit from the United Kingdom to the Falkland Islands. In this configuration, one radiometer was set to view the sea surface at an angle of 40° from nadir and the second to view the sky at 40° from zenith, the angle from which radiation would be reflected from a planar sea surface into the field of view of the sea view radiometer. TASCO data were averaged to a period of 5 s using the function provided on the instrument and logged to a Campbell Scientific CR10 data logger at a sample rate of 0.05 Hz and resolution of 0.025 K.

Spatially and temporally contemporaneous SSST was also measured by a SISTeR (Nightingale 1997) viewing the sea surface using near-identical[3] geometry to that of the TASCO instrument. The SISTeR data were collected using a narrowband (less than 1 μm)

TABLE 2. Weighted seawater emissivity ϵ computed for the TASCO THI-500L radiometer for different view angles ζ.

ζ (deg)	ϵ
0	0.98769
10	0.98767
20	0.98744
30	0.98686
40	0.98435
50	0.97667

[3] The SISTeR beam half-angle is 6.5°.

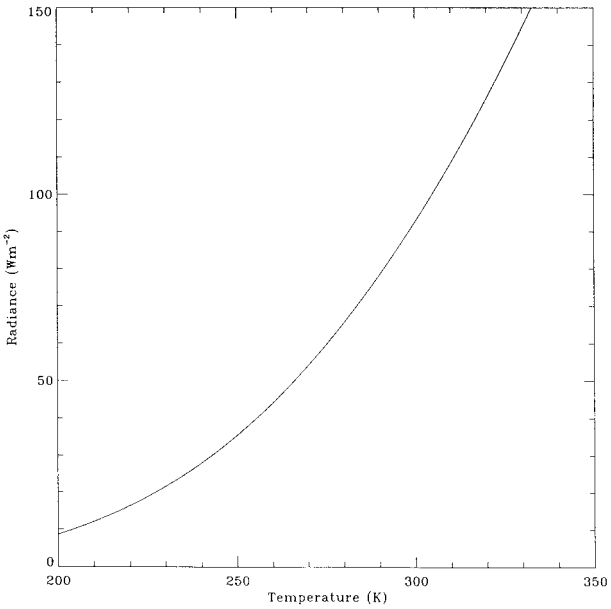

FIG. 4. The radiance to temperature relationship computed for the TASCO THI-500L radiometer integrated over the transmission profile shown in Fig. 1.

TABLE 3. Polynomial coefficients a_n for the TASCO THI-500L temperature T to radiance R relationship $R \Rightarrow T$ and radiance to temperature relationship $T \Rightarrow R$. The polynomial is of the form $y = a_0 + a_n \times x^n + \ldots$. * Error in fitted radiance: 0.01426%. ** Error in fitted temperature: 0.08047%.

a_n	$R \Rightarrow T$*	$T \Rightarrow R$**
a_0	−135.26027	165.20405
a_1	2.6586628	5.118575
a_2	−0.019156285	−0.1529919
a_3	5.6989092e-05	0.0034300275
a_4	−5.0308292e-08	−4.8940693e-05
a_5	9.5095291e-12	4.3401177e-07
a_6	−2.3088176e-09	—
a_7	6.7266478e-12	—
a_8	−8.2336320e-15	—

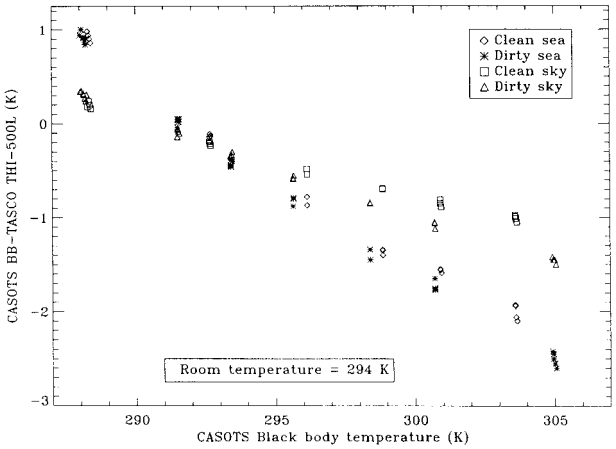

FIG. 5. Effect of foreoptics contamination by seawater on the calibration of both sky and sea view TASCO THI-500L radiometers during the ROSSA 1996 experiment. Curves show the calibration derived from each radiometer before (dirty) and after (clean) cleaning the instrument's foreoptics.

filter centered at 10.8 μm and a sample frequency of 1.25 Hz. A sea view was made between two sky view periods of 4 s acquired at the start and end of the sea view. A two-point internal blackbody calibration system together with the excellent thermal stability and high signal-to-noise characteristics of the SISTeR design assured a measurement accuracy of the order 0.1 K (Nightingale 1997).

Although the TASCO lenses were cleaned at regular intervals, contamination was inevitable and, unfortunately, the nature of the installation on the RRS *James Clark Ross* prevented daily recalibration of the TASCO instruments. However, after periods of particularly heavy weather both of the TASCO instruments were unmounted and recalibrated using a CASOTS blackbody (BB) unit. The data shown in Fig. 5 show calibration data obtained for each instrument before and after contamination had been cleaned from the radiometer's foreoptics using distilled water and alcohol. In this plot, the CASOTS BB temperature has been plotted as a function of the residual difference between the CASOTS BB and the TASCO radiometer output over a temperature range of 287–305 K. This plot highlights the degradation of calibration due to foreoptics' contamination and, in particular, how the calibration of the sky radiometer is now significantly different from the sea view instrument. Further, foreoptics' contamination introduces errors that increase as the temperature difference between the calibration target and instrument (which is at room temperature) increases. This error is difficult to detect because it is small at temperatures close to the ambient instrument temperature (which will be similar to the SSST). Although a typical TASCO temperature–SSST difference of ± 2 K will limit this error to less than 0.2 K, in the context of satellite validation and the investigation of the BSST–SSST difference this value is significant.

Using the clean optics calibration data obtained prior to and during the ROSSA 1996 experiment, together with the ϵ values of Table 2, we calculated the SSST using the TASCO radiometers for the duration of the ROSSA 1996 experiment. These data, averaged to 1-min intervals and plotted against the corresponding SISTeR data, are presented in Fig. 6.

The comparison for the entire (day and night) ROSSA 1996 dataset is shown in Fig. 6a, which reveals the TASCO SSST to have mean bias of −0.37 K and rms deviation of 0.23 K relative to the SISTeR data. These data have been further subdivided into day- and nighttime periods and are presented in Figs. 6b and 6c, respectively. The largest TASCO deviations are found during the daytime periods for which the bias is −0.47 K and rms is 0.25 K. The nighttime data show better agreement with the SISTeR data having a bias of −0.27 K and an rms deviation of 0.14 K, although there are slightly less data.

Figure 6 includes measurements made over a wide spectrum of environmental conditions and regions. In the configuration used, the TASCO radiometers were totally exposed to the effects of direct solar radiation, direct spray, rain, aerosol, and wind. In some cases the combined effect of these elements was severe, and significant contamination of the instrument's foreoptics occurred. In this sense, the small rms differences between the TASCO and SISTeR radiometers add confidence to the use of the TASCO THI-500L radiometer to determine SSST in the harsh conditions typical of the marine environment. Some of this difference is due to the different temporal sampling periods of the SISTeR and TASCO systems where rapid changes in the surface wave field and cloud cover (e.g., broken cumulus) relative to the SSST measurements can be important. Some of the data were taken during very calm sea conditions and include measurements made when considerable areas of the sea surface were contaminated by surface slick material. In these cases the appropriate value for the ϵ of seawater remains undefined, and the corresponding effect on measured

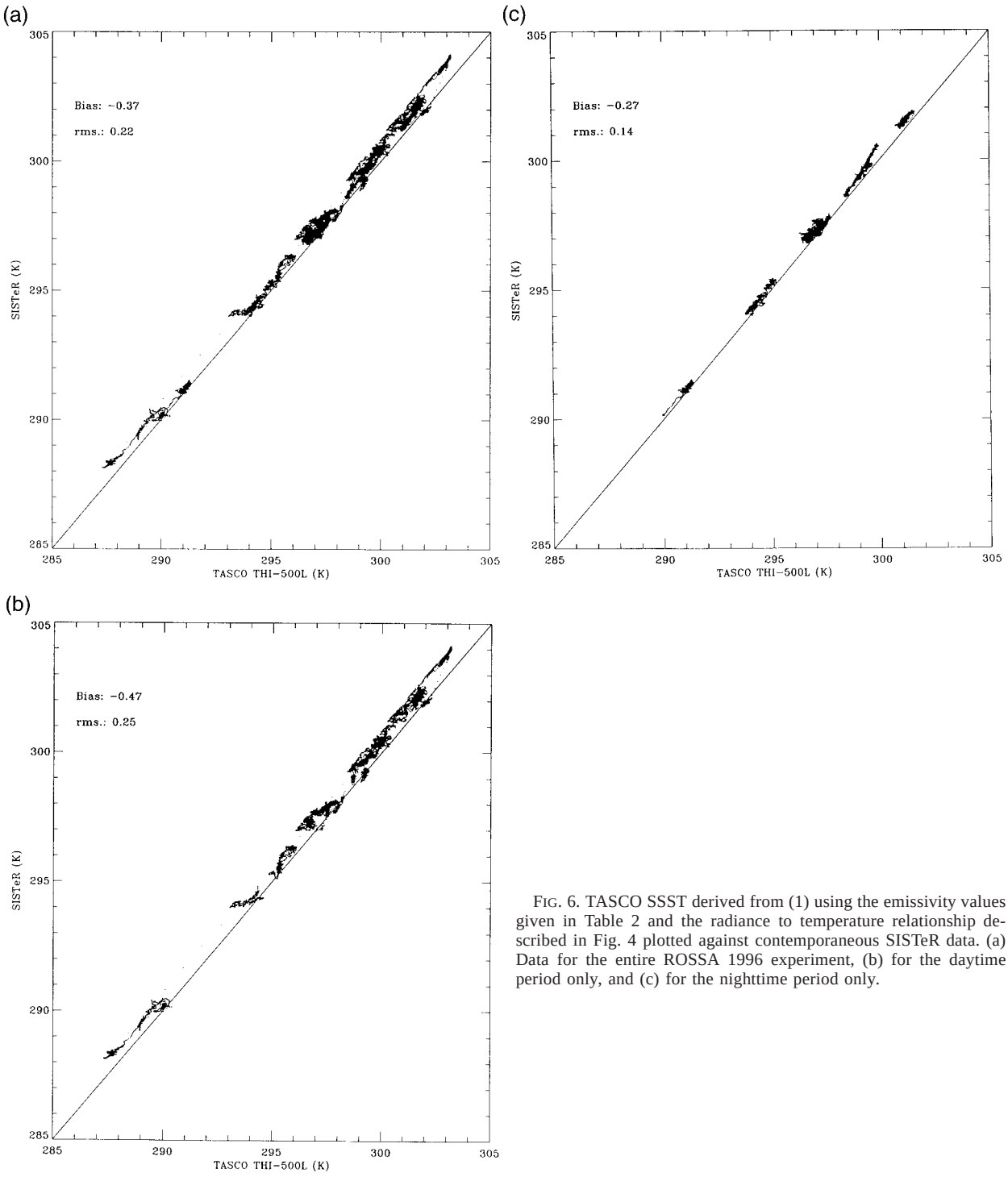

FIG. 6. TASCO SSST derived from (1) using the emissivity values given in Table 2 and the radiance to temperature relationship described in Fig. 4 plotted against contemporaneous SISTeR data. (a) Data for the entire ROSSA 1996 experiment, (b) for the daytime period only, and (c) for the nighttime period only.

SSST for the different spectral regions of the SISTeR and TASCO radiometers is unclear.

However, the TASCO data show a cool bias relative to the SISTeR data, which is of interest. This may be the result of errors associated with real differences between the actual infrared transmission properties of the TASCO filter and the detector windows and the ideal profile given in Fig. 1 together with errors in the calculated values of seawater emissivity. Some of this bias may also be attributed to the real differences between the SISTeR and TASCO spectral wavebands; the penetration depth (*e*-folding depth) for a radiometric mea-

surement made at wavelength of 10.8 μm is about 10 μm, whereas for a wavelength of 8.3 μm the depth is about 22 μm. The skin layer can support a strong temperature gradient that typically results in a cooler surface layer than the water immediately beneath, which does not agree with these observations. However, as the TASCO radiometers were unprotected during ROSSA 1996, the data presented in Fig. 6 should be considered a ''worst-case'' deployment scenario that provides an upper bound on the accuracy of the TASCO radiometers.

c. Results from the 1995 MUBEX

The Mutsu Bay Experiment (MUBEX) is a Japanese–U.K. collaborative project (Donlon et al. 1995) established to validate satellite-derived SSST and pseudo-BSST data from both the ERS–ATSR and NOAA Advanced Very High Resolution Radiometer (AVHRR) instruments. As part of this process, MUBEX explored the use of alternative techniques to measure radiometric SSST using thermal infrared camera systems and solid-state radiometers. During the MUBEX 1995 experiment two TASCO THI-500L radiometers were used to measure the SSST from the R/V *Diani Misago* in Mutsu Bay, northern Honshu Island, during July and August 1995.

The TASCO THI-PRL units were thermally insulated from the effects of solar warming using a specially constructed polystyrene jacket that was coated in reflective foil to minimize solar warming. The radiation entering the TASCO radiometers was collected using mirrors attached to the THI-PRL head. The mirror units greatly facilitate accurate positioning of the radiometer field of view and were supplied by TASCO Japan Co. Ltd. The MEUs were housed in a separate waterproof box, and the entire assembly was installed on a specially constructed instrument platform attached to the bow of the R/V *Diani Misago.* In this configuration, the sea surface was viewed at an angle of 15° and the sky at the complimentary zenith angle, and the sea view radiometer footprint had a diameter of 0.75 m. BSST measurements were made using a conductivity–temperature–depth (CTD) profiler suspended at a depth of 1 m so that the sensor head was in clear water. The CTD data are accurate to better than ± 0.02 K.

One-minute averages of the SSST were derived from the TASCO radiometers using Eq. (1), together with the appropriate values for the emissivity of seawater and the radiance to temperature relationship data described in Tables 2 and 3. These data have been plotted together with the BSST measured at a depth of 1 m in Fig. 7a. The data shown represent a typical transect leg made during MUBEX 1995 when the R/V *Diani Misago* was traveling slowly at a speed of approximately 2 m s^{-1}. The average wind speed during this transect was 4.0 m s^{-1}, and the mean solar flux was 407 W m^{-2}. Cloud cover was 5 oktas, consisting of thicker cumulus and

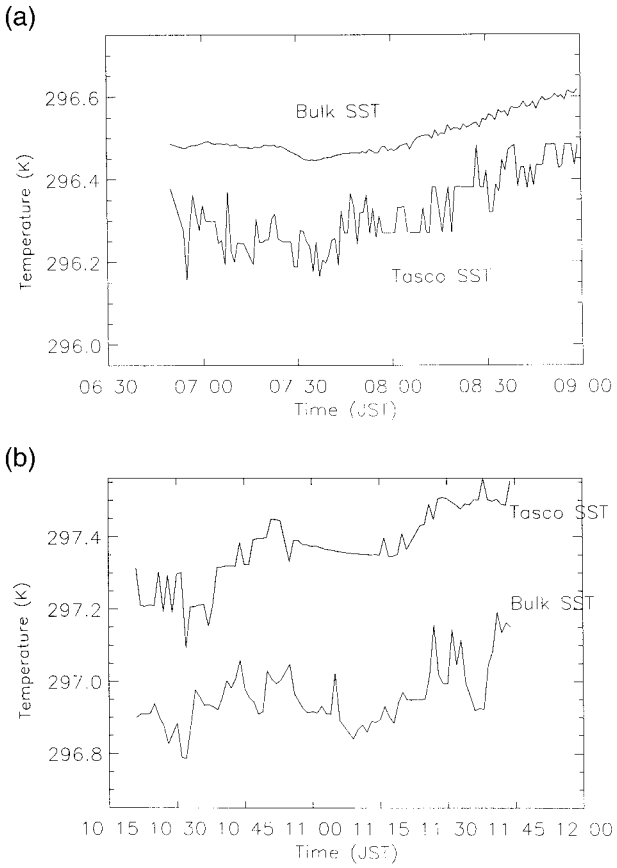

FIG. 7. (a) One-minute averages of TASCO THI-500L SSST from (1) and BSST at 1 m made on 22 August 1995 during the MUBEX 1995 experiment made prior to the maximum insolation period. (b) Similar observations made on the 23 August 1995 during low wind speed during the onset of a diurnal thermocline.

stratocumulus cloud. The TASCO SSSTs follow the subsurface BSSTs extremely well, having a mean cool bias of approximately 0.25 K, which is in good agreement with the magnitude expected of the BSST–SSST difference. The peak-to-peak variability of the TASCO SSST was approximately 0.2 K and was primarily due to real changes in the SSST forced by changes in the heat flux due to wind speed variability. Figure 7b shows TASCO-derived SSST and contemporaneous BSST at 1 m for a later period during the following day. The average wind speed for this transect was less than 2.0 m s^{-1} and the average solar flux was higher (greater than 755 W m^{-2}). Although the cloud cover was 7 oktas, most of this consisted of thin cirrostratus and haze. In this case the TASCO SSSTs are apparently warmer than the BSST observations and a ''warm'' skin prevails. However, this does not preclude the existence of a cool skin because the 1-m BSST measurement is below the depth of maximum diurnal warming in the very upper layers of the sea surface. More importantly, these data highlight the apparent sign-change variability of the BSST–SSST difference ΔT when referenced to a sub-

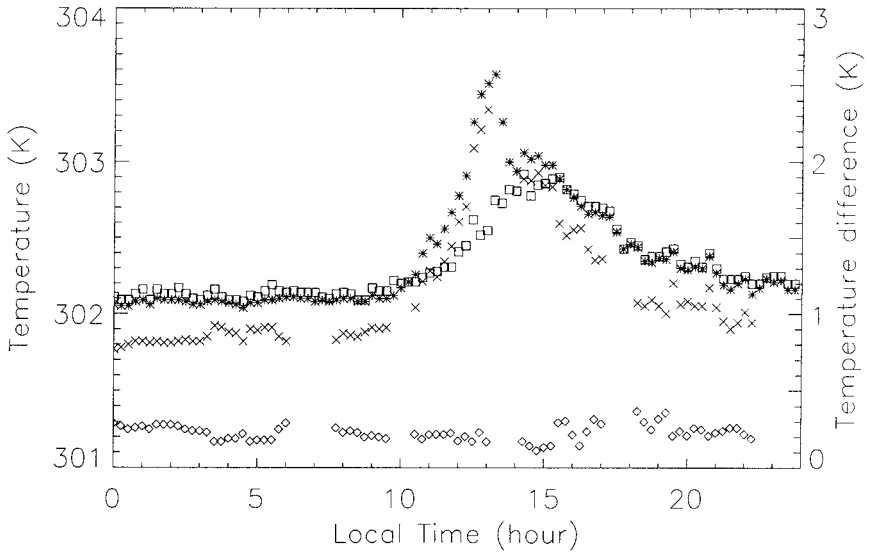

FIG. 8. Tropical Indian Ocean sea surface temperature measured from the R/V *Franklin* during 29 August; towed thermistor (*), TASCO (×), thermosalinograph (□). The difference between the thermistor and the TASCO is also shown (◇).

surface BSST measurement and clearly demonstrate the need to measure a detailed vertical profile of the upper 1 m of the sea surface when investigating ΔT or validating satellite SSST using BSST data.

d. Measurements in the tropical Indian Ocean

During August and September 1996 the R/V *Franklin* undertook a cruise to study the freshwater and heat budgets of the tropical Indian Ocean. On 29 August the *Franklin* operated over a small area of the Indian Ocean bounded by latitudes of 3.15° and 3.40°S and longitudes of 92.6° and 92.9°E. The weather throughout the day was fine with a maximum wind speed during the 24 h of less than 5 m s^{-1}.

The BSST was measured using a thermosalinograph that sampled the water from approximately 1 m below the surface and a towed thermistor that sampled the surface temperature at a depth between 0.01 and 0.05 m. SSST measurements were made using a TASCO THI-500L radiometer mounted near the bow and viewing the water surface at an angle of 45° to nadir ahead of the ship's bow wave. The TASCO head was installed inside an insulated tube covered with reflective foil, and the control unit was protected separately in a waterproof canister; both were shaded from direct sunlight. The analog output was recorded on the same logger as the towed thermistor; both signals were sampled every 10 s and averaged over 15-min periods. The TASCO was calibrated using a blackbody cavity twice during the cruise. The analog output (as logged) was found to be linear over the temperature range 277–307 K, and at ambient temperature (300–306 K) the calibration changed imperceptibly (i.e., less than a few milli-Kelvins) over the 8-day period between calibrations.

As only one radiometer was available for this experiment, it was not possible to continuously measure the sky temperature. Instead, the sea view radiometer was used to obtain periodic sky measurements that have been taken to be representative of the conditions throughout the measurement period. The appropriate value for the emissivity of seawater has been taken from Table 2 and used to derive the SSST from the TASCO sea and sky measurements, as described in previous sections.

The temperatures measured by the towed thermistor, the thermosalinograph, and the TASCO are shown in Fig. 8. The thermistor clearly shows the solar heating of the upper ocean layers between 1000 and 1300 LT. During this period vertical mixing was inhibited due to light winds of less than 1 m s^{-1}. The thermosalinograph also shows the heating but at a much reduced rate. The wind increased to nearly 3 m s^{-1} at 1330 LT, and the result of increased mixing can be seen in the temperature measurements. After 1500 LT the thermosalinograph and thermistor show good agreement. Prior to 1000 LT the thermosalinograph gives a measurement that is approximately 0.04 K warmer than the towed thermistor.

The TASCO measurements shown in Fig. 8 are consistently about 0.25 K ± 0.1 K cooler than the thermistor. The measurements thus indicate a skin layer that is cooler than the bulk temperature just below the surface by about 0.25 K. This is true even throughout the formation of the diurnal heat layer and its destruction due to the increased wind mixing after 1330 LT. Some of the fluctuations in the difference between the thermistor and the TASCO can be related to cloud cover as measured by broadband radiometers and the vertical movement of the towed thermistor in thermally stratified waters. However, the data do show the consistency and

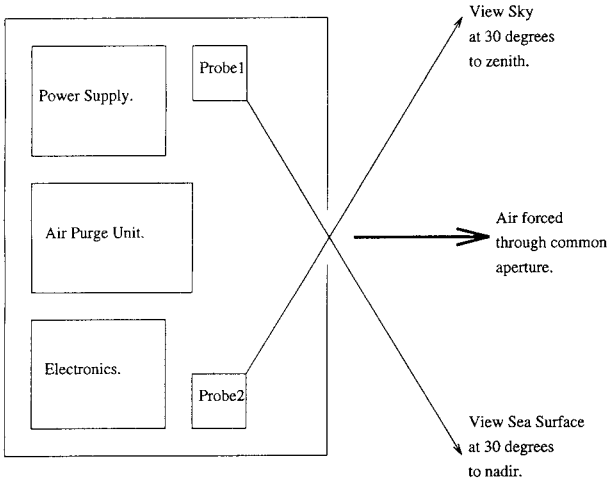

FIG. 9. A schematic diagram showing the basic design of the ship of opportunity sea surface temperature radiometer (SOOSR).

sensitivity of the TASCO measurements when used to measure SSST.

e. Results from Southampton University Department of Oceanography Ferry Experiment (SUDOFEX)

The aim of SUDOFEX is to provide a high quality dataset for the study of the oceanic thermal skin temperature deviation and for the validation of satellite SSST measurements by collecting a repeat ocean–atmosphere dataset from a ship of opportunity (the MV *Val de Loire*, a cross-Channel ferry vessel that sails regularly between the United Kingdom and France). For this particular experiment, two TASCO THI-500L radiometers were incorporated into the ship of opportunity radiometer system (SOOSR) developed by the University of Southampton Department of Oceanography for the measurement of SSST.

The SOOSR uses a rugged steel enclosure to protect the TASCO radiometers from rain, spray, condensation, and solar warming. The box was maintained at a positive pressure by a simple fan unit, as shown in Fig. 9. This was intended to prevent spray or rain from entering the instrument and contaminating the radiometer's foreoptics. The first radiometer views the sea surface, while a second views the sky at the complementary angle through a common exit aperture. To minimize the effects of solar warming, reflective paint has been applied to the exterior of the enclosure. The internal temperature of the SOOSR backplate is continuously monitored and is taken to be representative of the TASCO radiometer head temperatures that are unable to provide a measurement themselves.

During SUDOFEX, the SOOSR viewed the sea surface at an angle of 30° to nadir and the sky at 30° to the zenith. Both TASCO radiometers used in the SOOSR were calibrated before and after SUDOFEX using a CASOTS BB unit, which showed that the calibration of the two TASCO instruments had not changed over the 10-day deployment. BSST was measured on the MV *Val de Loire* by two precision rhodium–iron (ReFe) thermometers installed in dedicated glands on the large (diameter of 0.75 m) engine intake pipe, 3 m inboard of the seawater intake port and before the ship's pumps at a depth of 4 m. Warming of the seawater was negligible in this configuration, and BSST measurements were accurate to better than 0.05 K. BSST varied from 281 K in coastal regions to 293 K in the middle of the English Channel, which is typical for this region and season.

SOOSR SSST data were derived following the same procedure as for the ROSSA experiment using the appropriate value for seawater ϵ based on the geometry of the *Val de Loire* installation. The distribution of the residual between the SOOSR and contemporaneous SISTeR SSST is presented in Fig. 10, and shows that the SOOSR has a slight positive bias relative to the SISTeR data. We note that these data are found predominantly at the lower temperatures characteristic of the English Channel coastal region. Visual observations report large surface slick features present on the sea surface in these regions, which add uncertainty to the results and may explain the positive bias shown in Fig. 10. However, even in these conditions, extreme differences of less than 0.3 K exist between the SISTeR and SOOSR SSST observations. The low values for the mean and rms difference between the SOOSR and the SISTeR data demonstrate the effectiveness of the environmental protection offered by the SOOSR instrument enclosure.

5. Discussion

Although the spectral response of the TASCO radiometer is larger than the narrow bandwidths utilized by satellite radiometer systems (which require precise channel differences in order to account for the effect of the earth's atmosphere), if the appropriate correction for the nonblackness of the sea surface is made, the TASCO radiometer will measure the same temperature as the satellite, which is the thermal skin temperature. Laboratory calibration data presented in Fig. 2 clearly demonstrate that the TASCO THI-500L infrared radiometer system is capable of delivering measurements of the required accuracy for the validation of current satellite SSST measurements and the investigation of the BSST–SSST difference if the instrument's foreoptics remain uncontaminated. The relatively low cost together with the simplicity and acceptable accuracy offered by the TASCO THI-500L radiometers facilitates this type of measurement that previously required the purchase of expensive research-quality instrumentation.

The field deployments described in section 4 show different approaches to the measurement of SSST using TASCO THI-500L radiometer systems. In the case of the Indian Ocean and MUBEX 1995 deployments,

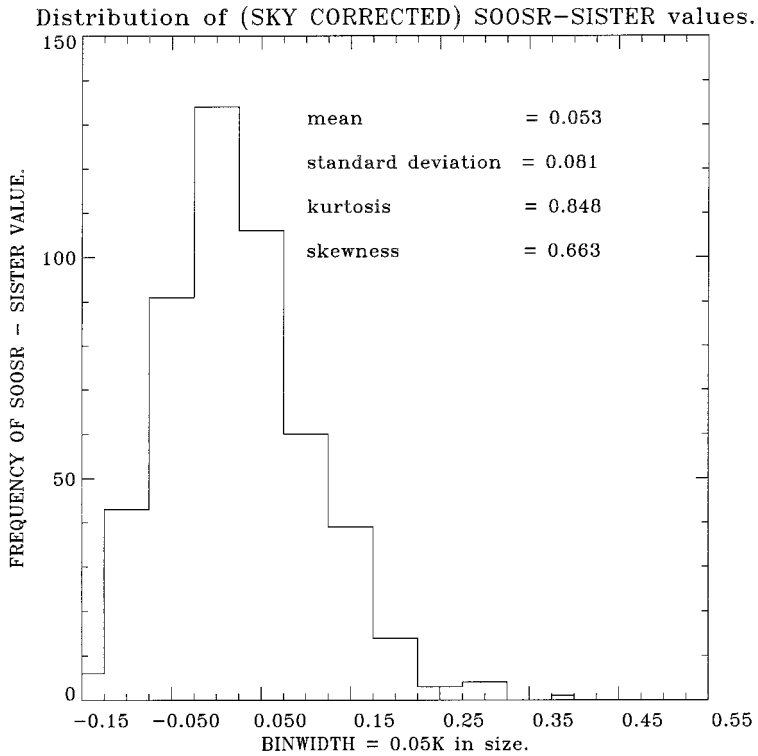

FIG. 10. The residual distribution of SOOSR SSST and contemporaneous SISTeR SSST observations collected during the SUDOFEX experiment. SOOSR SSST were derived from (1) using the emissivity values given in Table 2 and the radiance to temperature relationship described in Fig. 4.

where favorable environmental conditions prevail (i.e., calm sea and no rain), and visual inspection of the instruments is relatively easy and frequent, the TASCO foreoptics remained uncontaminated. The TASCO-derived SSSTs highlight the need to use SSST data for the validation of satellite BSST or SSST as opposed to the more traditional subsurface BSST measurements. In the case of the ROSSA 1996–AMT-3 experiment, the two TASCO radiometers were exposed to extremes of environmental conditions with little protection for a 6-week deployment. The small rms and bias differences shown in the comparison between the narrow spectral band SISTeR radiometer and the broader band TASCO THI-500L are thus remarkable and add confidence to the use of the TASCO instruments. Clearly, the effect of foreoptics contamination degrades the accuracy of the TASCO-derived SSST relative to the SISTeR observations and is most pronounced when comparing the SUDOFEX and ROSSA datasets. In the case of the SUDOFEX experiment, where a greater degree of protection was given to the TASCO radiometers, the excellent agreement with the SISTeR data confirms that the TASCO THI-500L radiometer system is capable of deriving accurate SSST measurements when deployed in an appropriate manner. The TASCO radiometers must remain uncontaminated by the effects of salt water, aerosol, and solar warming.

In all of the above field deployments, the sky view TASCO instrument was pointed to the region of the sky from which radiation would be directly reflected at the sea surface into the SIL radiometer field of view, assuming plane reflection at the sea surface. This procedure ignores the important effect of sea state and surface roughness, which may allow radiance from a much larger part of the sky to be reflected into the sea pointing radiometer field of view. In overcast or clear-sky conditions, although the sky radiance will vary due to the increasing atmospheric pathlength as the sky view radiometer view angle changes, this difference is generally small. However, in partially cloudy conditions a single point view of the sky may be unable to adequately sample the complicated and varied radiance contributions made by clear-sky regions and cloud bases at different heights. A narrowband hemispheric measurement of the integrated sky radiance might be a more appropriate measurement to use for accurate determination of downwelling sky radiation in these situations. However, this would require the development of a suitable wide-angle lens, substantially adding to the cost of the TASCO instrument. An alternative approach would be to ''scan'' the sky, as in the case of the SISTeR instrument or, in the case of the TASCO radiometers, by moving a sky view radiometer. This technique is limited as it will only sample the distribution of radiance contributions from

a single ''slice'' of the atmosphere. The recent work of Yoshimori et al. (1994, 1995) offers a more sophisticated approach relying on precision thermal infrared imaging cameras to make contemporaneous sea and sky views called statistically corrected ocean thermography (SCOT). These data are then combined using a statistical locational procedure to derive a corrected SSST. Unfortunately, the cost and difficulty of deploying such delicate instrumentation makes such a technique difficult to consider in an operational sense. It is clear from this discussion that more work in this area is required if radiometric measurement accuracy is to be significantly improved.

Another source of error to consider in the derived SSST measurement is the direct effect of solar radiation. This is noticeable when comparing the ROSSA day and night data presented in Figs. 6b and 6c. One explanation for these differences is the possibility that the TASCO transmission function has a shortwave ''leak'' and a direct solar contribution is made to the sea BT measurement via reflection. However, we note that the effect of direct reflected solar radiation across the broad spectral region used by the TASCO radiometers can make a significant contribution (Saunders 1967). In the case of direct contamination of the sky view radiometer, the error may lead to significantly raised sky temperatures, and an incorrect SSST will be derived. In the case of the sea view radiometer, especially during calm sea conditions, direct reflection at the sea surface can lead to significant errors; assuming a uniform sky BT of 230 K, which is specularly reflected into the sea radiometer field of view, we calculate that at an angle of 20° the reflected solar component can increase the measured sea BT by up to 1.7 K. A flat calm sea surface is rare and a more typical case of 10% contamination due to small surface waves, or when the sun is not directly ahead, leads to a potential increase in measured temperature of 0.2 K. While this error is small, it is still significant and care must be taken to dismiss these corrupted data from further analyses. One possibility would be to use a combination of solar elevation, ship heading, and a pyranometer to determine the likelihood of direct solar contamination.

The problems discussed above indicate that if the TASCO instrumentation is to be used with confidence for the validation of satellite SSST, then a regular and reliable calibration system is required together with some indication of the sea surface state, the amount of solar warming, and the wind speed. Accurate and reliable calibrations made using portable blackbody units such as the CASOTS blackbody are normally possible during research experiments. However, this is not possible during unattended deployments using volunteer ships of opportunity. The most reliable and effective approach in this case will be to include a simple calibration subsystem into any future instrument designed for use at sea together with an air purge system to prevent foreoptics contamination similar to that used in the SOOSR instrument. Two blackbody units are held at different temperatures that ideally straddle the actual SSST. In practice, one unit can be passive and remain at the ambient instrument temperature and a second unit actively heated. Such a system would allow a correction to be made for any contamination of the instrument foreoptics during autonomous deployments and is currently being developed by the authors.

6. Conclusions

A low-cost infrared radiometer system suitable for the measurement of sea surface skin temperature measurements has been tested in the laboratory and in the field. Laboratory calibrations of the TASCO THI-500L radiometer, using a precision blackbody cavity maintained in different environmental temperature conditions, show that these radiometers have an acceptably small (less than ± 0.2 K) environmental temperature dependency when the instrument's foreoptics are kept clean. Using the normalized transmission response function of the TASCO radiometer together with published values of seawater emissivity, we have calculated the spectrally weighted emissivity and radiance to temperature relationship for the TASCO THI-500L radiometer. These data are required to derive the SSST from simultaneous brightness temperature observations of the sea surface and sky made by two TASCO radiometer units.

A comparison between SSST derived from a precisely calibrated SISTeR and the SSST derived using TASCO radiometers when unprotected from the effects of solar warming and foreoptics contamination show rms differences of ± 0.14 K and a bias of -0.27 K at night. During the day, the rms increases to ± 0.25 K and the bias to -0.47 K, which is probably related to the effect of solar radiation significantly warming the TASCO radiometers, the effect of direct solar contamination, or errors in the TASCO THI-500L transmission functions. These data can be considered to represent a ''worst-case'' deployment where the effect of foreoptics' contamination and solar warming have significantly degraded the TASCO observations.

Data obtained from environmentally protected TASCO radiometers when compared to SISTeR data show that the TASCO radiometers are capable of providing SSST data that agree with the SISTeR data and an rms and bias of better than 0.1 K. These results demonstrate the need to protect the TASCO radiometers from the harsh marine environment. When such environmental protection can be given, these relatively inexpensive instruments could form the basis for a concerted large spatial- and temporal-scale global ship of opportunity measurement program required for the ongoing global validation of satellite-derived SSST measurements. Such measurements are a prerequisite to ensure that a long-term, precision, high quality, climatic SSST dataset is derived from the synergistic combination of different

satellite infrared radiometer datasets available from both current and future satellite radiometer systems.

Acknowledgments. The authors would like to thank Captain J. Burgen and ship's company of the RRS *James Clark Ross* during the 1996 ROSSA–AMT-3 experiment. We wish to acknowledge the support of the British Antarctic Survey Ice and Climate division, especially John Turner and the National Environmental Research Council of the United Kingdom. SUDOFEX was supported by NERC Grant GT12/94/3OP/46. Thanks go to Paul Hincke of Brittany Ferries and the captain and crew of the MV *Val de Loire*; Gary Fisher, Southampton University Department of Oceanography Technical Services; and the SUDOFEX meteorological observation volunteers. The authors would like to thank Ian Helmond and the crew of the R/V *Franklin* for assistance with the collection of the Indian Ocean data. We would like to thank Ryuzo Yokoyama and Sumio Tamba for their support and assistance in collecting the MUBEX data used here. Craig Donlon acknowledges the support of the Royal Society for participation in the 1995 MUBEX experiment. We would also like to thank Alistair Jenkins and Olivier Pinte for their helpful comments and discussion during the preparation of this paper. This work was supported in part by NASA research Grant NAGW-1110.

REFERENCES

Bale, A. J., 1997: AMT-3 cruise report, Plymouth Marine Laboratory, Plymouth, United Kingdom, 102 pp.

Donlon, C. J., 1997: Radiometric Observations of the Sea Surface and Atmosphere: 1996 cruise report, Colorado Center for Astrodynamics Research (CCAR), University of Colorado, Boulder, Colorado, 44 pp.

——, and I. S. Robinson., 1997: Observations of the oceanic thermal skin in the Atlantic Ocean. *J. Geophys. Res.,* **102,** 18 585–18 606.

——, and ——, 1998: Radiometric validation of the *ERS-1* ATSR average sea surface temperature in the Atlantic Ocean. *J. Atmos. Oceanic Technol.,* **15,** 82–115.

——, I. Parkes, and R. Yokoyama, 1995: Mubex 1995 experimental plan, Mubex special report 1, Dept. Earth Obs. Science, University of Leicester, United Kingdom, 57 pp.

Downing, D., and D. Williams, 1975: Optical constants of water in the infrared. *J. Geophys. Res.,* **80,** 1656–1661.

Edwards, T., and Coauthors, 1990: The along track scanning radiometer—Measurement of sea-surface temperature from *ERS-1*. *J. British Interplanet. Soc.,* **43,** 160–180.

Emery, W. J, C. J. Donlon, and Y. Yu, 1996: Wind speed forcing of the bulk-skin sea surface skin temperature difference, (abstract). *Eos, Trans. Amer. Geophys. Union,* **77** (Fall meet. suppl.), 342.

Grassl, H., and H. Hinzpeter, 1975: The cool skin of the ocean. WMO GATE Rep. 14. [Available from World Meteorological Organization, Case Postale 2300, CH-1211 Geneva 2, Switzerland.]

Kent, E., T. Forrester, and P. K. Taylor, 1996: A comparison of the oceanic skin effect parameterizations using ship-borne radiometer data. *J. Geophys. Res.,* **101,** 16 649–16 666.

Masuda, K, T. Takashima, and Y. Takayama, 1988: Emissivity of pure and seawaters for the model sea surface in the infrared window regions. *Remote Sens. Environ.,* **24,** 313–329.

Nightingale, T. J., 1997: The scanning infrared sea surface temperature radiometer (SISTeR). Rutherford Appleton Laboratory, Chilton, United Kingdom, 30 pp.

Revercombe, H. E., F. A. Best, R. G. Dedecker, T. P. Dirkx, R. A. Herbsleb, R. O. Knuteson, J. F. Short, and W. L. Smith, 1993: Atmospheric emitted radiance interferometer (AERI) for ARM. Preprints, *Fourth Symposium on Global Change Studies,* Anaheim, CA, Amer. Meteor. Soc., 46–49.

Saunders, P. M., 1967: Aerial measurement of sea surface temperatures in the infrared. *J. Geophys. Res.,* **72,** 4109–4117.

Saurez, M., W. J. Emery, and G. Wick, 1997: The OPHIR calibration radiometer for multi-channel measurements of skin sea surface temperature. *J. Atmos. Oceanic Technol.,* **14,** 243–253.

Schlüssel, P., H. Y. Shin, W. J. Emery, and H. Grassl, 1987: Comparison of satellite derived sea surface temperatures with in situ skin measurements. *J. Geophys. Res.,* **92,** 2859–2874.

——, W. J. Emery, H. Grassl, and T. Mammen, 1990: On the bulk skin temperature difference and its impact on satellite remote sensing of sea surface temperature. *J. Geophys. Res.,* **95,** 13 341–13 356.

Smith, W. L., and Coauthors, 1997: Observations of the infrared radiative properties of the ocean—Implications for the measurement of sea surface temperature via satellite remote sensing. *Bull. Amer. Meteor. Soc.,* **77,** 41–51.

Thomas, J. P., and J. Turner, 1995: Validation of Atlantic Ocean surface temperatures measured by the *ERS-1* along track scanning radiometer. *J. Atmos. Oceanic Technol.,* **12,** 1303–1312.

Watts, P. D., M. R. Allen, and T. J. Nightingale., 1996: Wind speed effects on sea surface emission and reflection for the along track scanning radiometer. *J. Atmos. Oceanic Technol.,* **13,** 126–141.

Yokoyama, R., and S. Tanba, 1991: Estimation of sea surface temperature via AVHRR of *NOAA-9*—Comparison with fixed buoy data. *Int. J. Remote Sens.,* **12,** 2513–2528.

Yoshimori, K., I. Kazuyoshi, and Y. Ichioka, 1994: Thermal and reflective characteristics of a wind-roughened water surface. *J. Opt. Soc. Amer.,* **11,** 1886–1893.

——, ——, and ——, 1995: Optical characteristics of a wind-roughened water surface: A two-dimensional theory. *Appl. Opt.,* **34,** 6236–6247.

Zappa, C. J., 1997: Test of OPHIR calibration bucket using infrared imagery. Applied Physics Laboratory, University of Washington, Seattle, Washington, 12 pp.

Závody, A. M., C. T. Mutlow, and D. T. Llewellyn-Jones, 1995: A radiative transfer model for sea surface temperature retrieval for the along-track scanning radiometer. *J. Geophys. Res.,* **100,** 937–952.